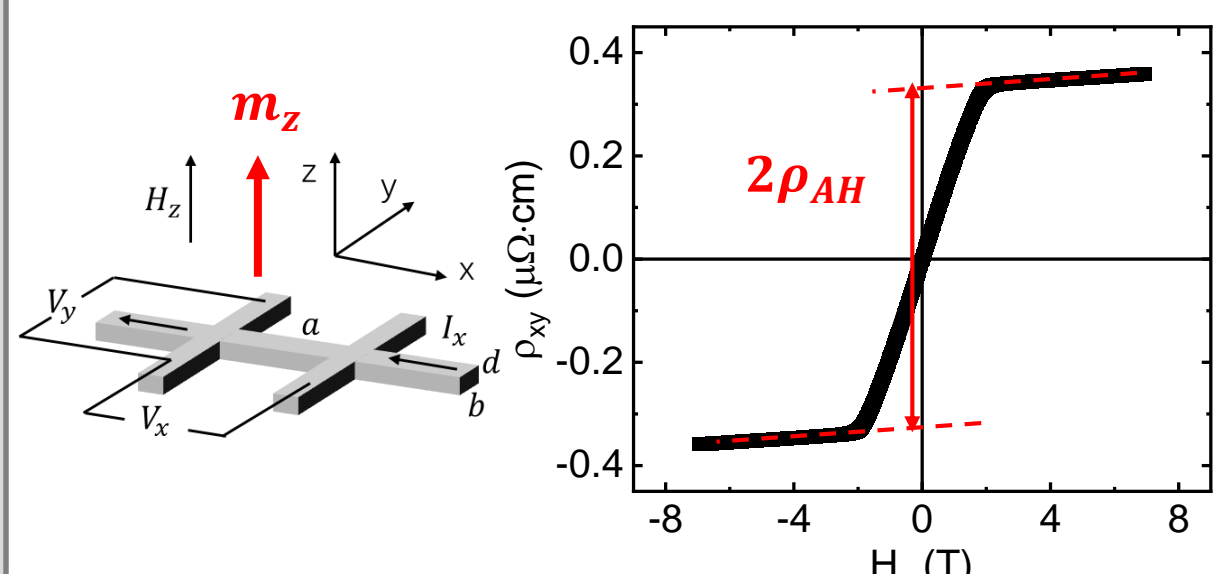


Introduction

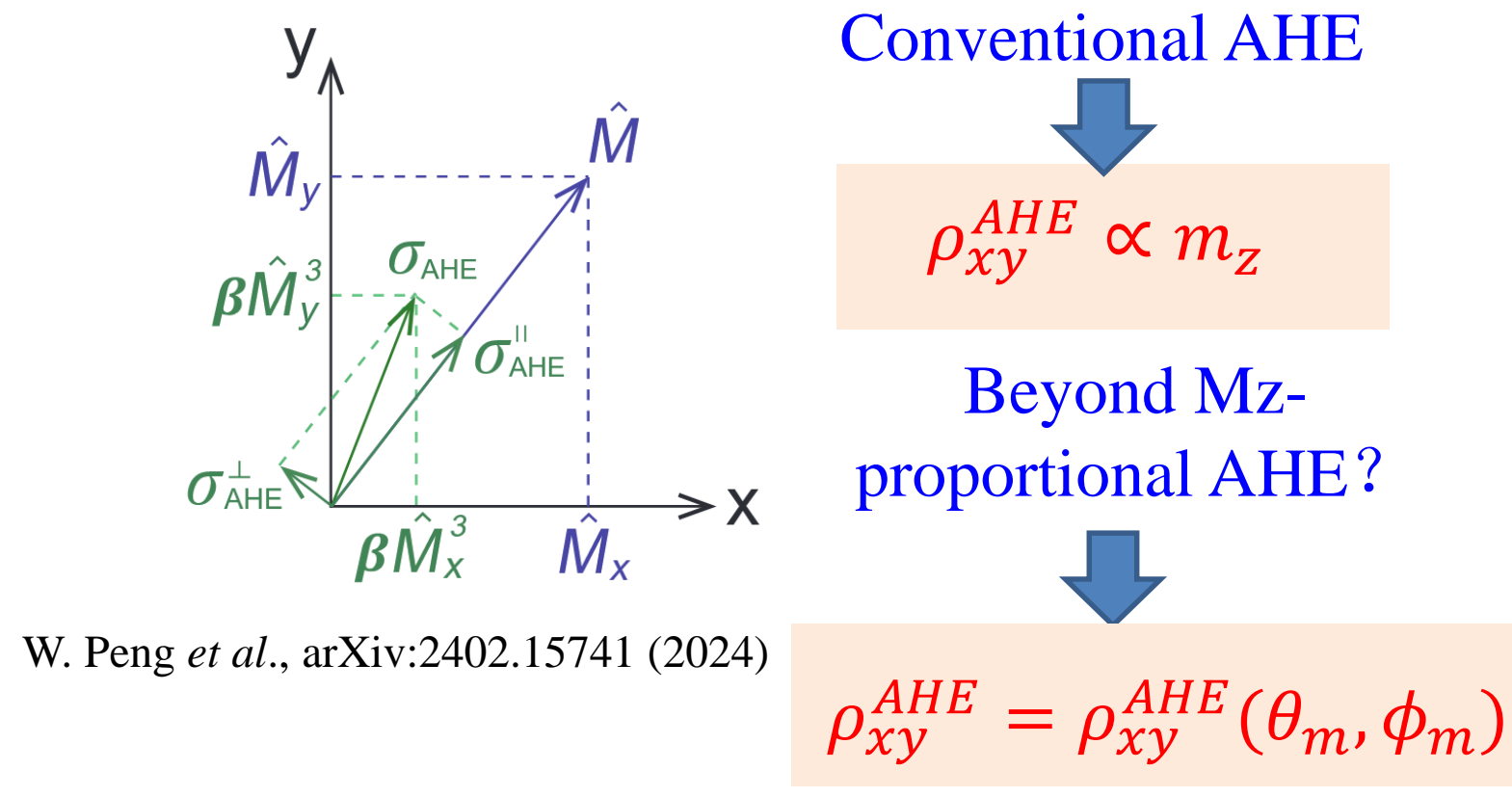
Anomalous Hall effect (AHE)



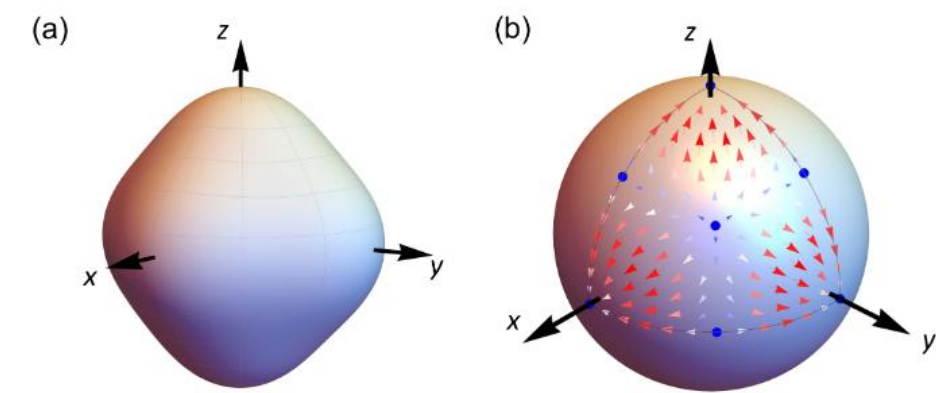
$$\rho_{xy} = \frac{V_y}{I_x} = R_H H_z + \rho_{AH} m_z$$

Ordinary Hall Anomalous Hall

AHE always proportional to Mz?



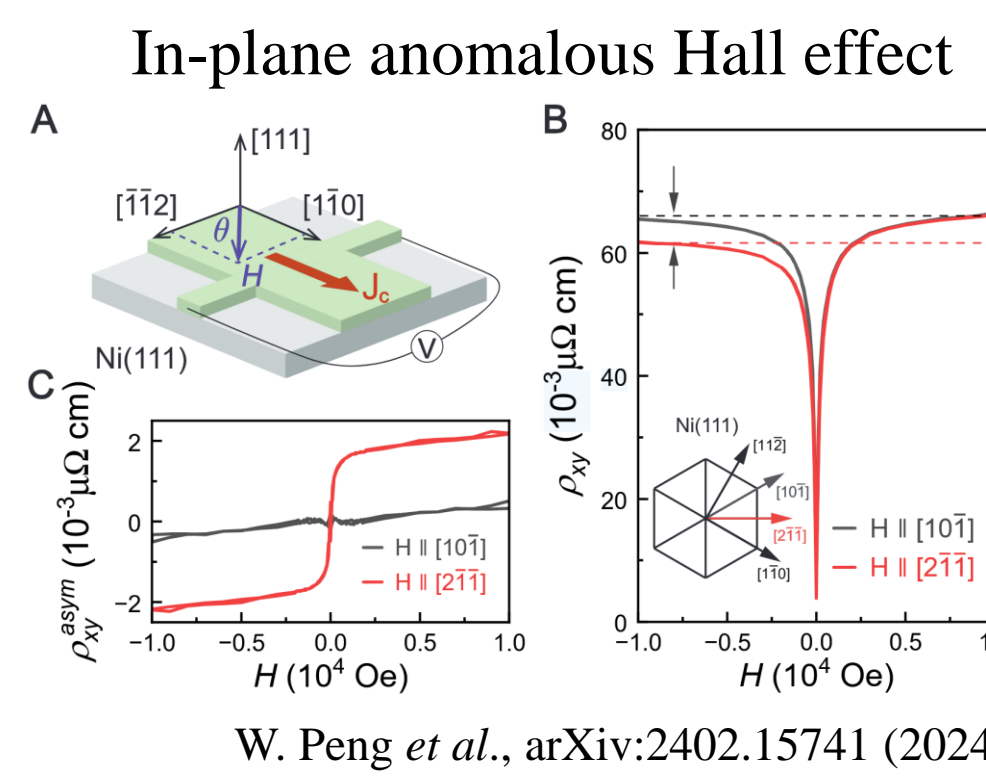
High-order AHE from multipolar response



$$\sigma_i^H = \alpha \hat{M}_i + \beta \hat{M}_i^3$$

High order Spin-orbit coupling
High order Spin-dependent transport

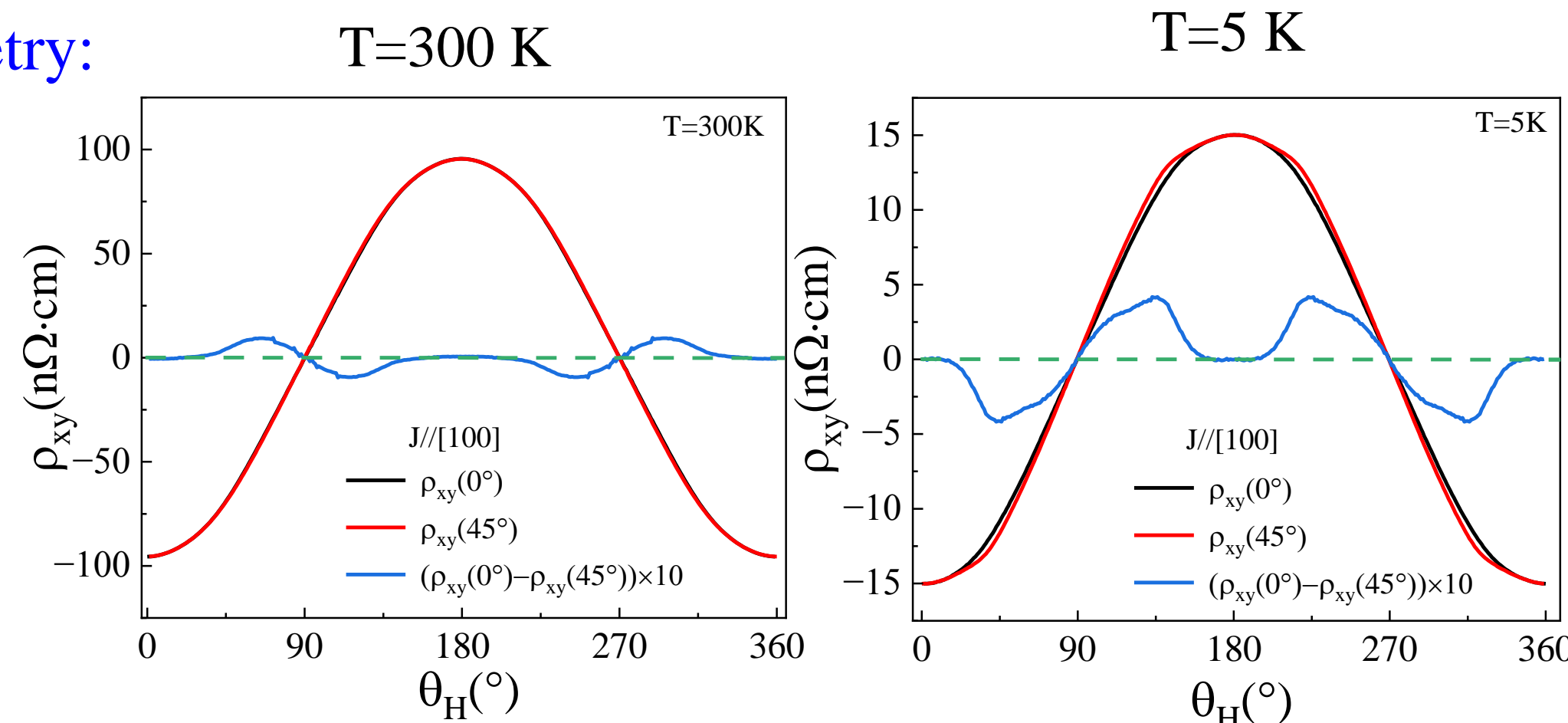
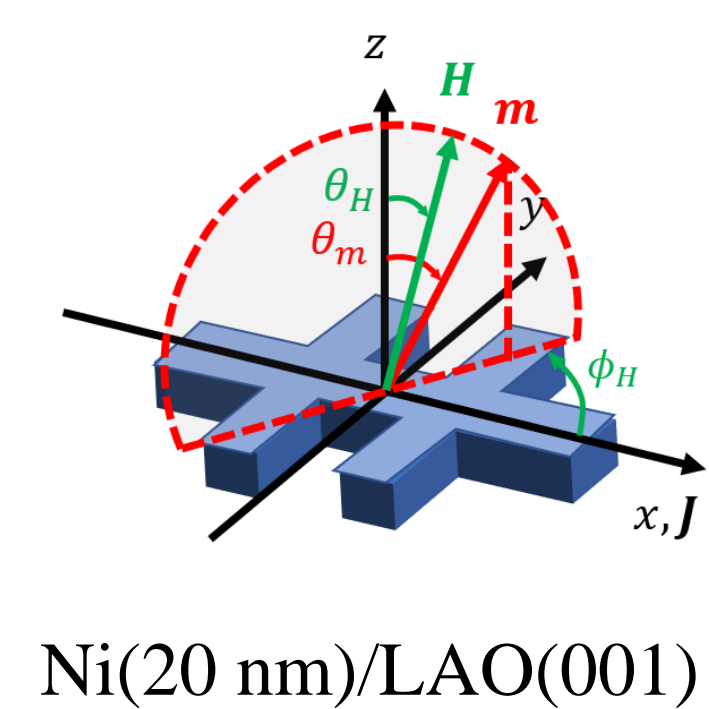
In-plane AHE: evidence beyond Mz response



Can high-order AHE harmonics carry in-plane crystalline anisotropy?

Observation of anisotropic angular-dependent AHE

Measurement geometry:

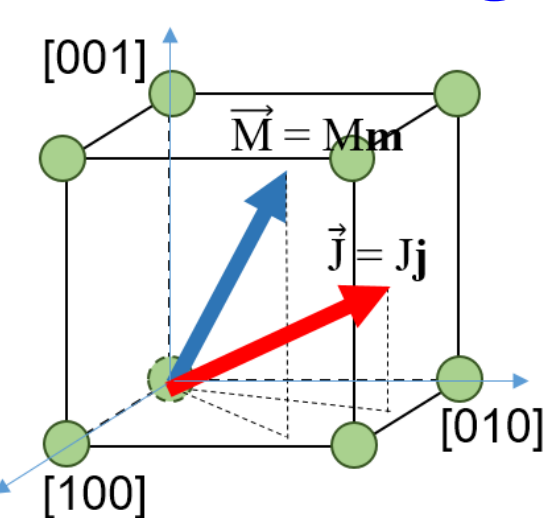


$$\rho_{xy}^{AHE}(\theta_m, 0^\circ) \neq \rho_{xy}^{AHE}(\theta_m, 45^\circ)$$

AHE contains an in-plane-sensitive component

Temperature evolution of anisotropic high-order AHE

Phenomenological model of AHE based on crystal symmetry



From Ohm's law $E_i = \rho_{ij} J_j$, expansion of ρ_{ij} on \mathbf{m} :

$$\rho_{ij}(\mathbf{m}) = a_{ij} + a_{kij} m_k + a_{klmij} m_k m_l m_m + \dots$$

Onsager relation: $\rho_{ij}(\mathbf{m}) = \rho_{ji}(-\mathbf{m})$

Cubic crystalline symmetry

W. Döring, Ann. Phys. 424, 259 (1938)

$$\rho_{ij}(\theta_m, \phi_m, \phi_j) = \sum_k \rho_{2k+1}^{(0)} \cos((2k+1)\theta_m) + \sum_k \rho_{2k+1}^{(4)} \cos((2k+1)\theta_m) \cos(4(\phi_m + \phi_j))$$

High-order expansion of AHE

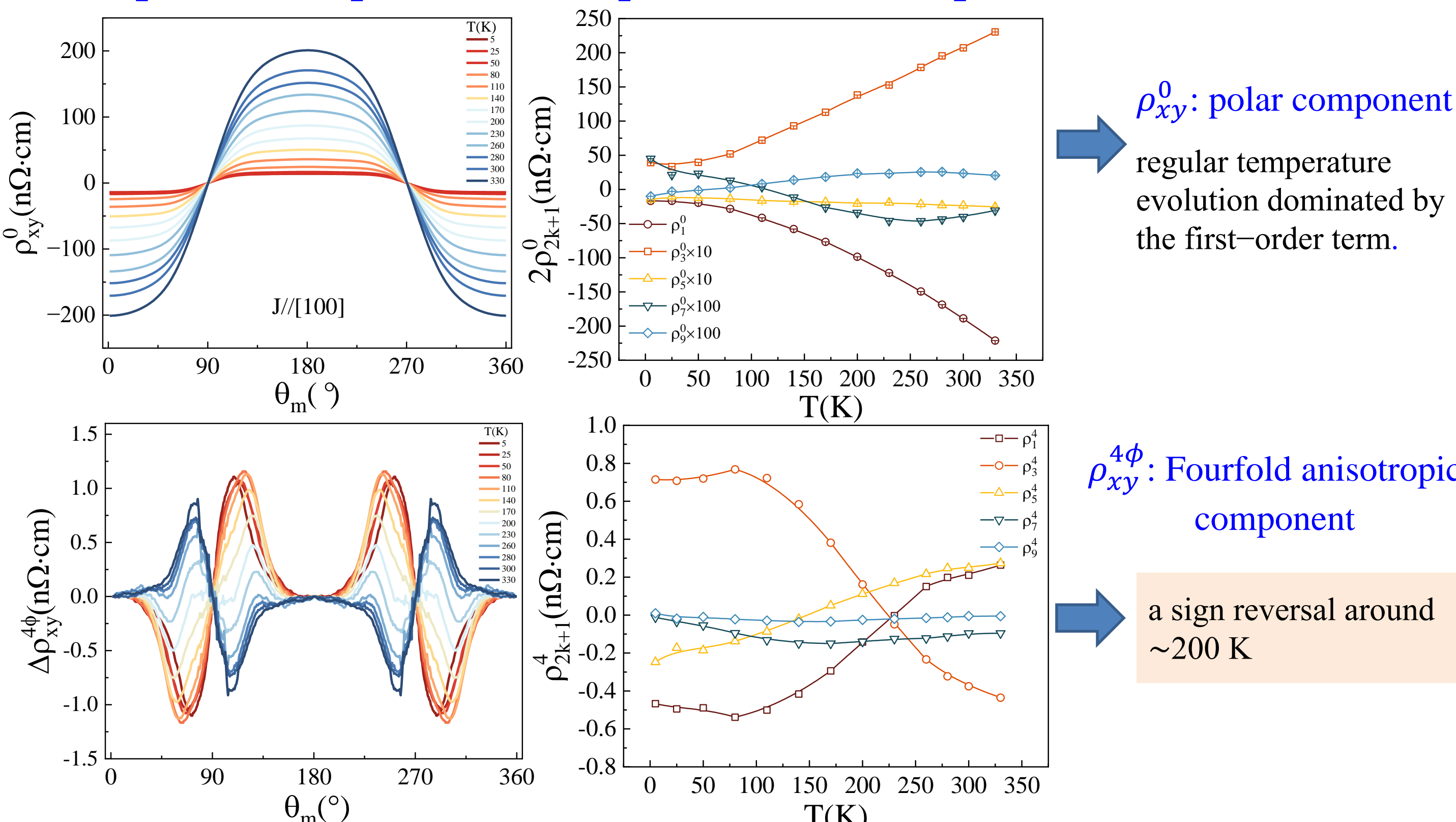
$$\rho_{xy}^{AHE}(\theta_m, \phi_m, \phi_j) = \rho_{xy}^0(\theta_m) + \rho_{xy}^{4\phi}(\theta_m, \phi_m, \phi_j)$$

$$\rho_{xy}^0(\theta_m) = \sum_k \rho_{2k+1}^{(0)} \cos((2k+1)\theta_m) \quad \rho_{xy}^{4\phi}(\theta_m, \phi_m, \phi_j) = \sum_k \rho_{2k+1}^{(4)} \cos((2k+1)\theta_m) \cos(4(\phi_m + \phi_j))$$

$$\Delta\rho_{xy}^0(\theta_m) = \rho_{xy}^{AHE}(\theta_m, \phi_m = 0^\circ, \phi_j = 0^\circ) - \rho_{xy}^{AHE}(\theta_m, \phi_m = 45^\circ, \phi_j = 0^\circ) = 2\rho_{xy}^0(\theta_m)$$

$$\Delta\rho_{xy}^{4\phi}(\theta_m) = \rho_{xy}^{AHE}(\theta_m, \phi_m = 0^\circ, \phi_j = 0^\circ) - \rho_{xy}^{AHE}(\theta_m, \phi_m = 45^\circ, \phi_j = 0^\circ) = 2\rho_{xy}^{4\phi}(\theta_m)$$

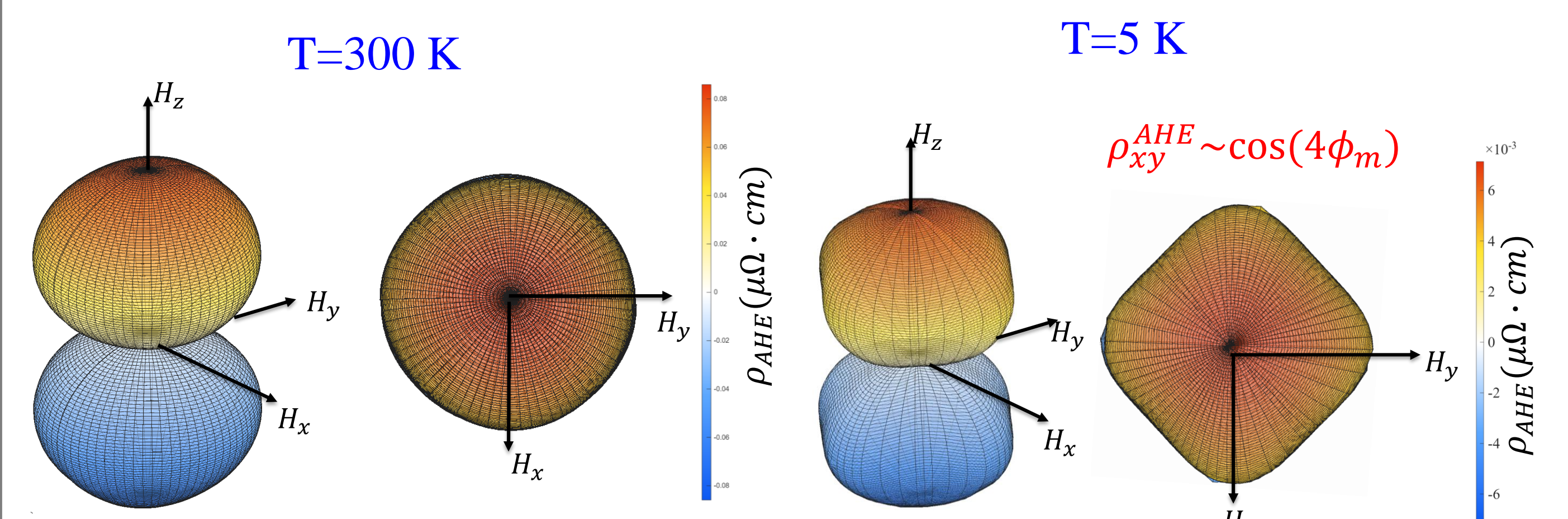
Temperature dependence of separated AHE components



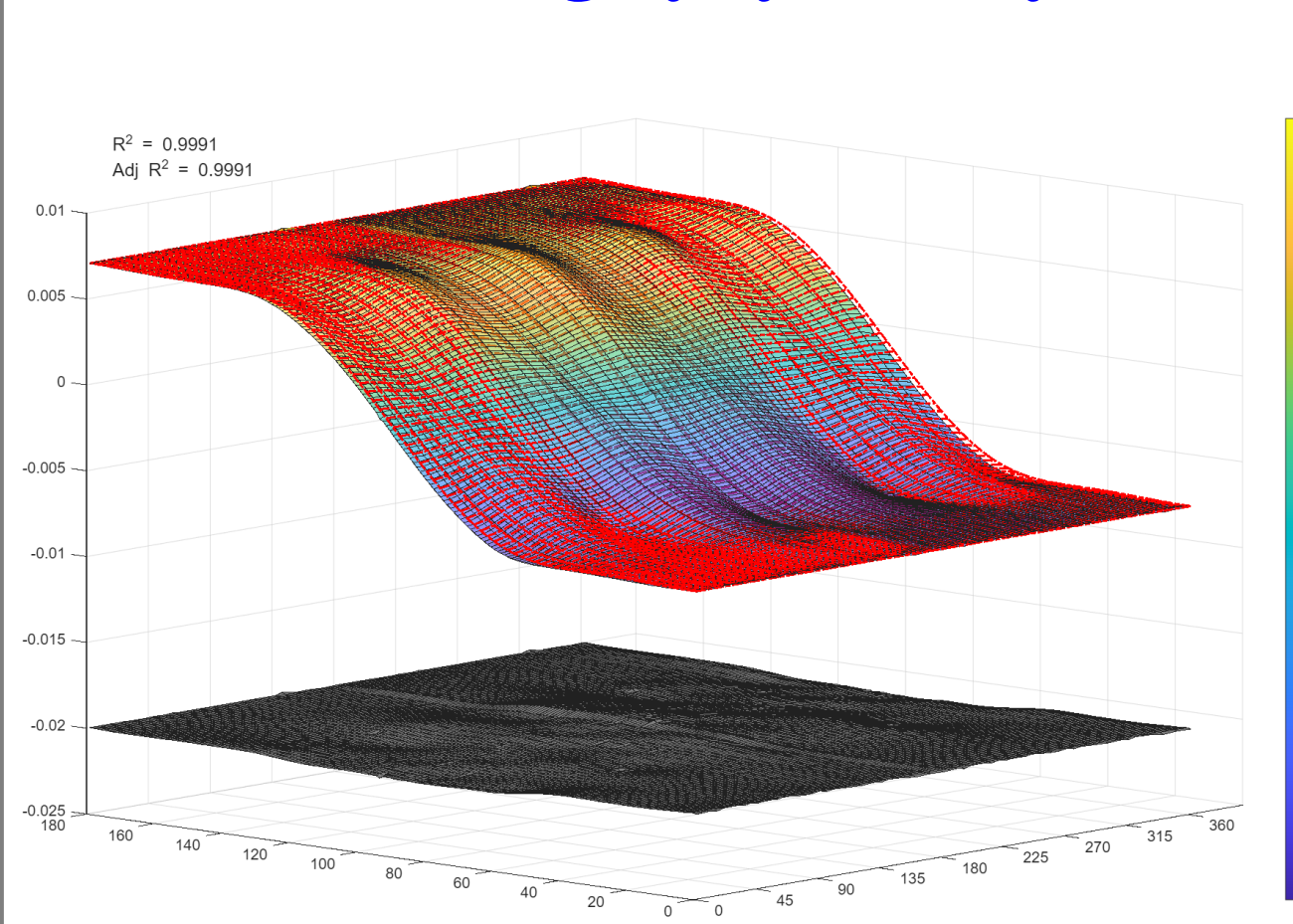
Polar and in-plane-sensitive AHE components exhibit distinct temperature evolution.

3D angular mapping of anisotropic AHE

3D full mapping of Ni(001) AHE

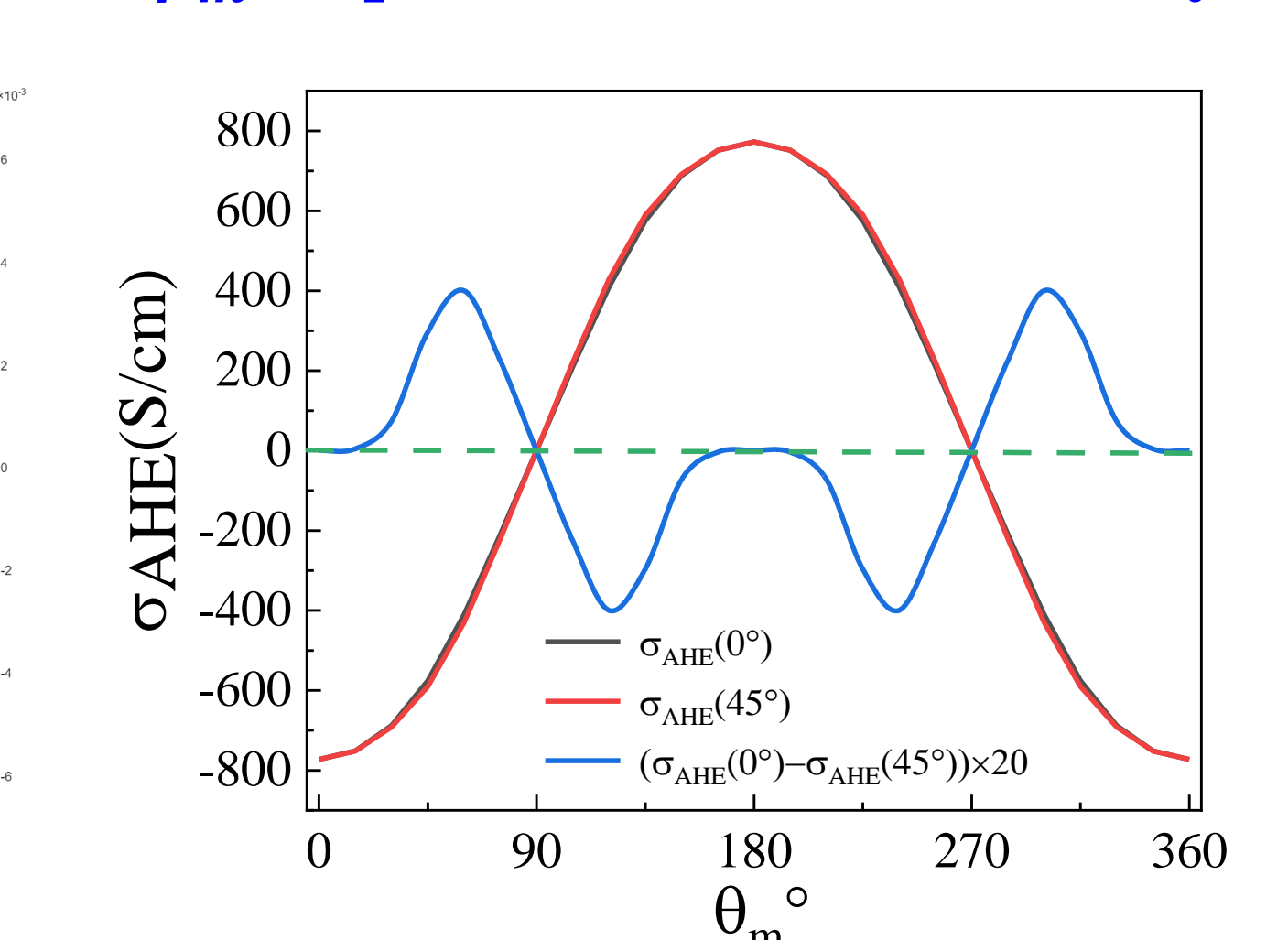


Global fitting by symmetry model



$$\rho_{xy}^{AHE} = \rho_{xy}^0(\theta_m) + \rho_{xy}^{4\phi}(\theta_m, \phi_m, \phi_j)$$

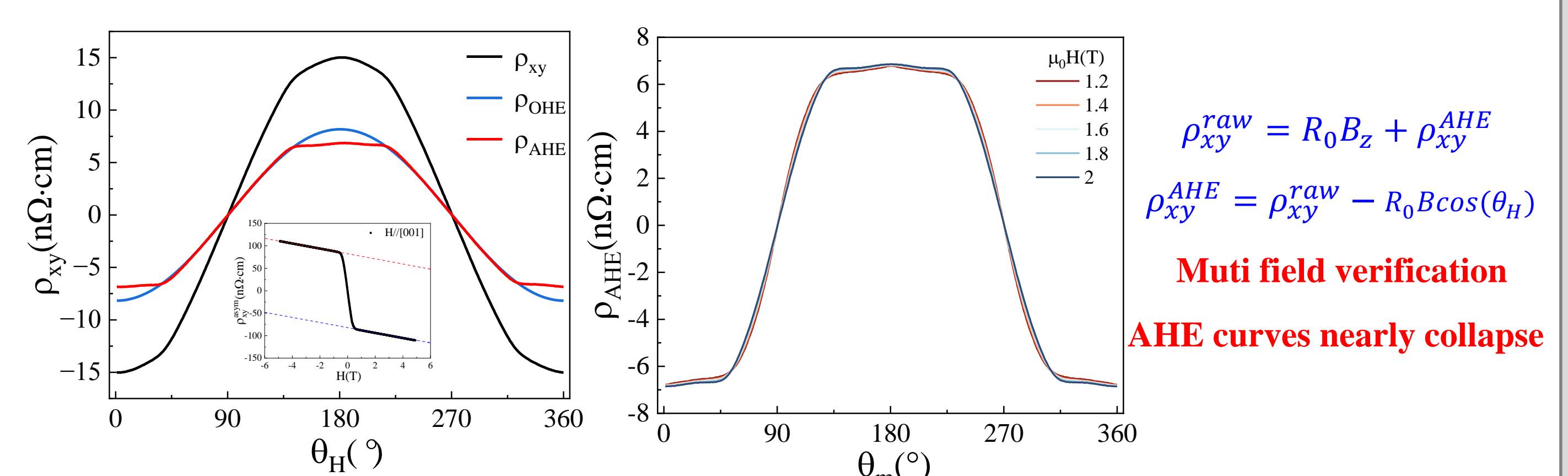
ϕ_m -dependent AHE confirmed by DFT



Full 3D angular mapping visualizes fourfold crystalline anisotropy in high-order AHE.

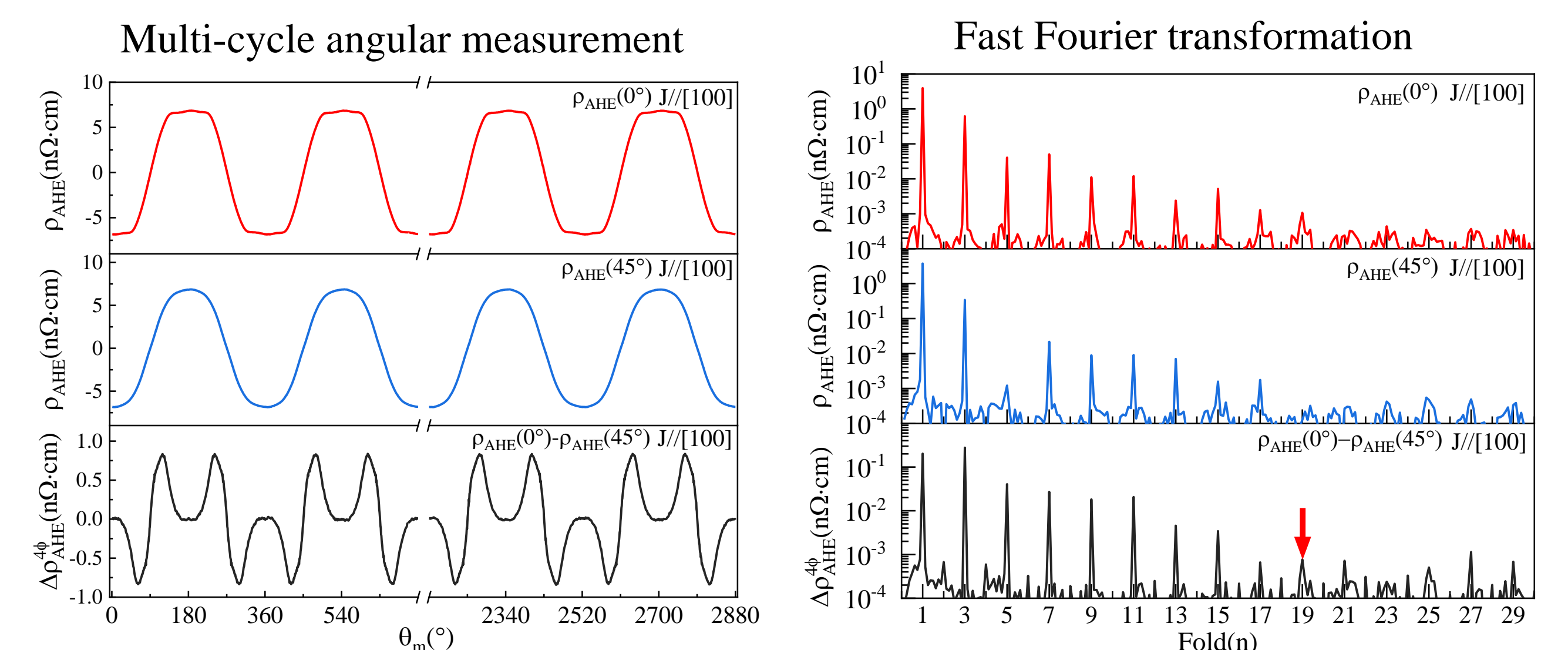
Extraction of intrinsic AHE and high-order harmonics

Ordinary Hall Subtraction



Fourier verification of high-order AHE

Up to 19-fold AHE



Beyond the conventional Mz picture.

OHE-subtracted AHE reveals robust odd-order harmonics up to 19 fold beyond the conventional Mz picture.

Summary

- High-order AHE harmonics up to 19th order in Ni(001)
- In-plane-sensitive AHE beyond the conventional Mz picture
- Fourfold anisotropy visualized by full 3D angular mapping
- Distinct temperature evolution of two AHE components